AJNR

MR of hemorrhage: a new approach.

R R Edelman, K Johnson, R Buxton, G Shoukimas, B R Rosen, K R Davis and T J Brady

AJNR Am J Neuroradiol 1986, 7 (5) 751-756
http://www.ajnr.org/content/7/5/751

MR of Hemorrhage: A New Approach

Robert R. Edelman[1]
Keith Johnson[2]
Richard Buxton[3]
Gregory Shoukimas[1]
Bruce R. Rosen[1]
Kenneth R. Davis[1]
Thomas J. Brady[1, 4]

Using a modification of the partial saturation (PS) pulse sequence, we developed an MR method that permits the acquisition of highly T1- and T2-weighted images of the head and body in as little as 10 sec. The PS images, which were acquired at 0.6 T in a series of six patients with acute and subacute hemorrhage, showed a striking reduction in the signal intensity of hemorrhagic lesions. This effect, which is related to bulk magnetic susceptibility variations, was either minimal or absent on conventional T1- and T2-weighted spin-echo (SE) images. Our results suggest that high-field systems are not needed in order to image acute and subacute hemorrhage.

It has recently been proposed that hemorrhage can be uniquely characterized on high-field images on the basis of magnetic susceptibility variations within the lesion [1]. These effects were not identified on low-field images [2–3]. If hemorrhage could be accurately identified only with high-field systems, this would of course provide a significant clinical advantage to these systems.

We have recently developed and implemented techniques for the rapid acquisition of T1- and T2-weighted images (Edelman RR, *Radiology*, submitted; Buxton R, *J Comput Assist Tomogr*, submitted). Using modifications of the partial saturation sequence, one can obtain these images in as little as 10 sec. It will be shown that, not only can one demonstrate magnetic susceptibility effects on intermediate field images, but that these images can be obtained in an order of magnitude faster than has previously been shown with high-field systems using conventional spin-echo techniques.

Subjects and Methods

Sixteen subjects were studied, including six patients with hemorrhagic lesions and 10 patients with nonhemorrhagic lesions by CT criteria. There were five patients with subacute hemorrhage: one patient with an angiographically occult arteriovenous malformation in the left pons; one patient with postpartum pituitary apoplexy imaged approximately 1 week postictus; one patient with a 4-week-old right parietal hemorrhage, presumed secondary to an underlying tumor; one patient with a 4-week-old left occipital hemorrhage, also presumed secondary to underlying neoplasm; and one patient status post liver transplant for cirrhosis with an intrahepatic hematoma resulting from a biopsy 4 weeks before the MR study. There was one acute right putaminal hematoma, imaged 15 hr from the ictus.

The 10 patients with nonhemorrhagic lesions included three patients with intrahepatic metastases (colon and breast primaries); two patients with intrahepatic cavernous hemangioma; two patients with nonhemorrhagic intracranial infarctions (brainstem, left middle cerebral artery territory); and three patients with nonhemorrhagic intracerebral gliomas.

MR was performed on a Technicare 0.6 T superconducting system. Patients were imaged with a variety of T1- and T2-weighted spin-echo (SE) or composite inversion-recovery spin-echo (IR) pulse sequences. T1-weighted sequences included SE 300/14, SE 500/20, and IR 1500/450/20. T2-weighted sequences included multiecho SE 2000/60,120, and SE 400/60,120. Acquisition time for the SE and IR images ranged from 5–15 min.

Received May 1, 1986; accepted after revision May 13, 1986.

This work was supported in part by a grant from Technicare Corp., Solon, OH, and by NIH grants 1K04 CA 00848-04 and 1ROI CA 40303-01.

[1] Department of Radiology, Massachusetts General Hospital, 32 Fruit St., Boston, MA 02114. Address reprint rquests to R. R. Edelman.

[2] Department of Neurology, Massachusetts General Hospital, Boston, MA 02114.

[3] Department of Radiologic Physics, Massachusetts General Hospital, Boston, MA 02114.

[4] Department of Medicine, Massachusetts General Hospital, Boston, MA 02114.

***AJNR* 7:751–756, September/October 1986**
0195–6108/86/0705–0751

T2-weighted partial saturation (PS) images were obtained in all subjects. The partial saturation sequence is similar to an SE sequence without a 180° radiofrequency (RF) refocusing pulse; the MR signal is read out as a gradient-echo, rather than a spin-echo [4]. T2-weighted images were obtained with small RF pulse angles (20°) and long TE (e.g., 30–120 msec). T1-weighted PS images were also obtained in five subjects using a large pulse angle (120°) and short TE (16 msec). For both acquisitions, four excitations and a TR of 100 msec were used (except for the TE = 120 msec acquisitions, where TR = 150 msec).

Liver images were acquired using 1.5-cm section thickness and one or two excitations (10 sec or 20 sec acquisition time) in conjunction with suspended respiration. Head images were acquired using 0.7-cm section thickness and four excitations (54 sec acquisition time). Head images were acquired on a 256 × 128 (frequency × phase) matrix; abdominal images were acquired on a 256 × 96 (frequency × phase) matrix in conjunction with a 1.33 × phase-encoding gradient zoom to produce equivalent spatial resolution to standard 128 projection acquisitions. All images were interpolated for display to a 256^2 matrix.

Two types of images were reconstructed from the same PS data set. Conventional images were reconstructed from the magnitude component of the data, where

$$\text{Magnitude component} = [(\text{real component})^2 + (\text{imaginary component})^2]^{1/2}.$$

In addition to the phase-insensitive magnitude images, phase-sensitive images were reconstructed from the real component of the data. In some cases, the echo was off-centered by a large first-order phase offset during reconstruction to produce "zebra-stripe" images [5]. One pair of bright and dark stripes is equivalent to a 360° phase shift.

Phantom studies were also performed to assess the differential sensitivity of SE and PS sequences to magnetic susceptibility effects. Magnetite (Fe_2O_3) is a superparamagnetic agent with a high magnetic susceptibility. By perturing local field homogeneity, it selectively shortens T2 and T2* (the time constant for proton dephasing under the influence of magnetic field inhomogeneities) but has minimal effect on T1 [6]. Sample tubes were filled with a 0.3% agar suspension containing 0, 33, 67 and 100 microgram/ml of albumin-coated magnetite microspheres (MAM; courtesy of Donald J. Widder, Molecular Biosystems, San Diego, CA). The tubes were imaged with an SE 200/20 sequence with two excitations, and with a PS 200/20 sequence with two excitations.

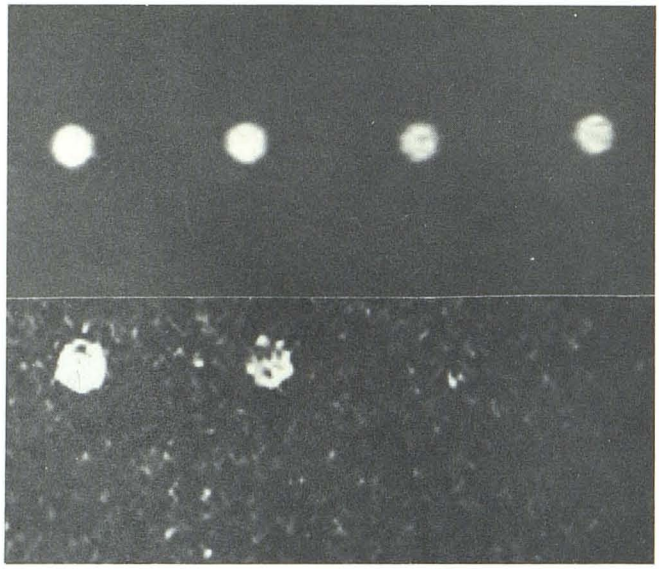

Fig. 1.—Differential sensitivity of spin-echo and gradient-echo images to magnetic susceptibility effects. Four tubes from left to right containing magnetite albumin microsphere (MAM) suspensions: agar; agar + 33 μg/ml MAM; agar + 67 μg/ml MAM; agar + 100 μg/ml MAM. Top images were acquired using an SE 200/20 sequence with two excitations; bottom images were acquired using a PS 200/20 sequence with two excitations. Note marked signal loss on gradient-echo acquisition in tubes containing magnetite.

Results

In the magnetite phantom study, the PS sequence was markedly more sensitive to the effects of the magnetic field inhomogeneities induced by magnetite than was an SE sequence acquired with the same TR and TE (Fig. 1). SE images showed all the tubes with at least moderate intensity. In contrast, only the tube containing agar without magnetite and the tube with the lowest MAM concentration could be seen on PS images. Since the echo time was the same on both images, the differential effect of magnetite must relate to shortening of T2*, rather than T2.

The acute putaminal hemorrhage was diffusely hyperdense on CT images; however, there was a more focal region that measured 9 H higher attenuation than the remainder of the hemorrhage (Fig. 2A). On T1-weighted SE images, the hemorrhage was isointense to gray matter (Fig. 2B). On T2-weighted SE images, a magnetic susceptibility effect was suggested by a subtle hypointense posterior border and mottled central hypointensity (Figs. 2C and 2D). T1-weighted PS images showed mild central hypointensity (Fig. 2E). These images showed greater signal in blood vessels, due to flow enhancement, than comparable T1-weighted SE images. T2-weighted PS images showed a very pronounced hypointense halo as well as marked central hypointensity, consistent with a magnetic susceptibility effect from hemorrhage (Figs. 2F and 2G).

Phase-sensitive zebra-stripe reconstructions directly showed the phase shifts associated with the magnetic susceptibility effects (Fig. 2H). A particularly large phase shift was noted in the region of greatest hypointensity on magnitude images (Fig. 2F), which corresponded with the focal area of increased density on CT images. This may represent a higher concentration of blood, perhaps at the site of origin of the bleeding.

Nonacute hemorrhages showed regions of hyperintensity on T1-weighted SE and PS images, presumably secondary to paramagnetic methemoglobin (Figs. 3–5). In one case there was no definite evidence of a magnetic susceptibility effect even on heavily T2-weighted SE images (Fig. 3B). However, PS images showed a prominent hypointense halo (Figs. 3D and 3E). In another case, a hypointense halo was noted on T2-weighted SE images, surrounding a hyperintense central region (Fig. 4B). On T2-weighted PS images, the entire lesion appeared hypointense (Fig. 4C). Phase-sensitive images showed prominent phase shifts in the region of the lesion

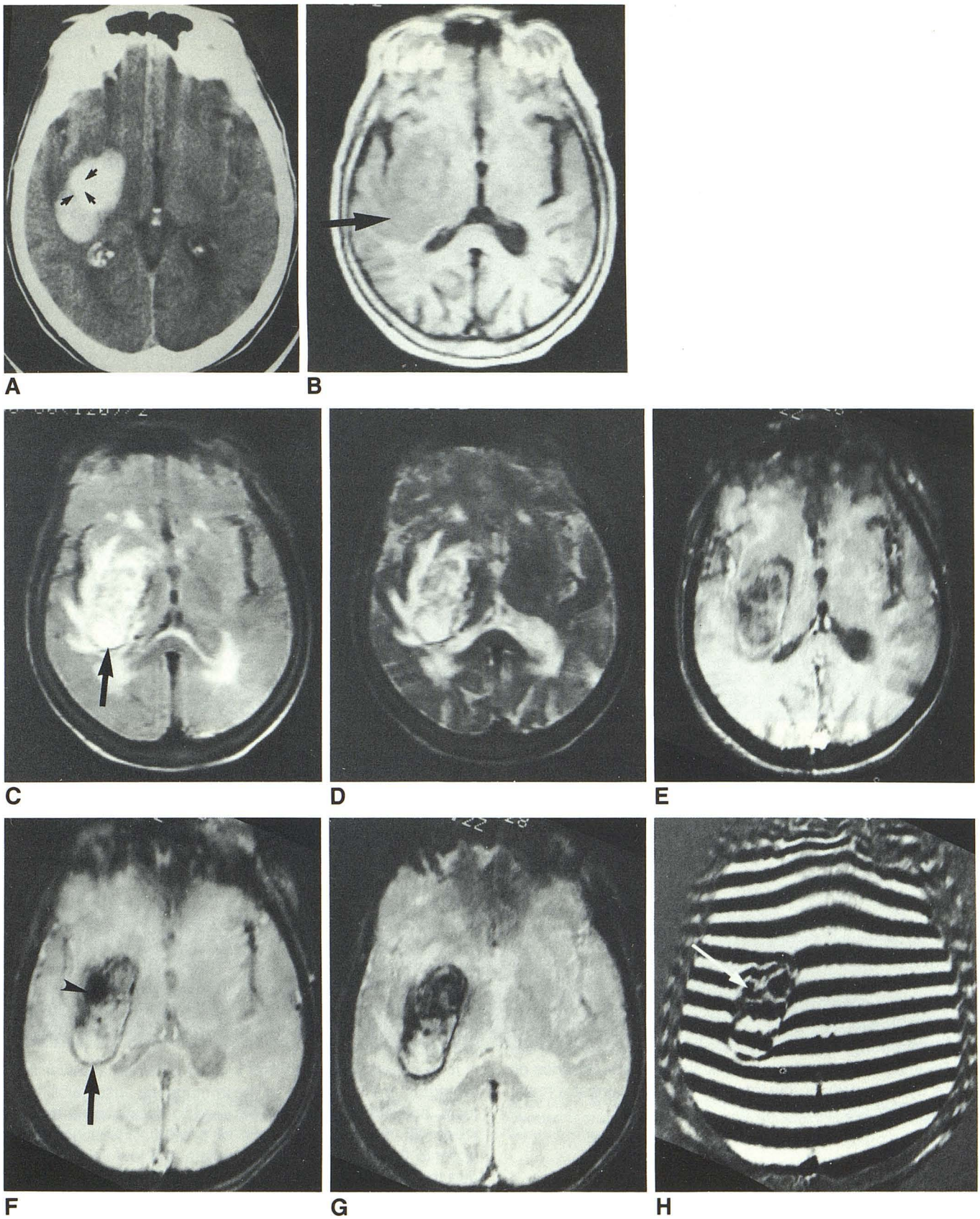

Fig. 2.—Patient with acute right putaminal hemorrhage. **A**, CT scan done shortly before MR examination shows hyperdense hemorrhage with more focal region (*arrows*) measuring 9 H higher attenuation than rest of hemorrhage. **B**, T1-weighted SE image shows nonspecific lesion (*arrow*) isointense to gray matter. **C**, T2-weighted SE image (TE = 60 msec) shows hyperintense lesion. There is a suggestion of a low-intensity halo (*arrow*). Mild central hypointense area is similar in intensity to white matter. Findings raise possibility of hemorrhage. **D**, More T2-weighted SE image (TE = 120 msec) shows similar findings to **B. E**, T1-weighted PS image (TE = 16 msec) shows hypointensity within lesion, in contrast to **A.** Note marked degree of flow enhancement compared with SE image. **F**, Moderately T2-weighted PS image (TE = 30 msec) shows definite low-intensity halo (*arrow*); also seen is a focal area of marked hypointensity (*arrowhead*) that corresponds to area of increased density in **A. G**, More T2-weighted PS image (TE = 50 msec) shows pronounced hypointense halo as well as a markedly hypointense area that is much lower in intensity than white matter. Diagnosis of hemorrhage is unequivocal. **H**, Phase-sensitive zebra-stripe reconstruction shows marked phase shifts in halo due to magnetic susceptibility gradient at junction of hemorrhage and brain. Also note focally increased phase shift (*arrow*) in region of focal hypointensity seen in **E.**

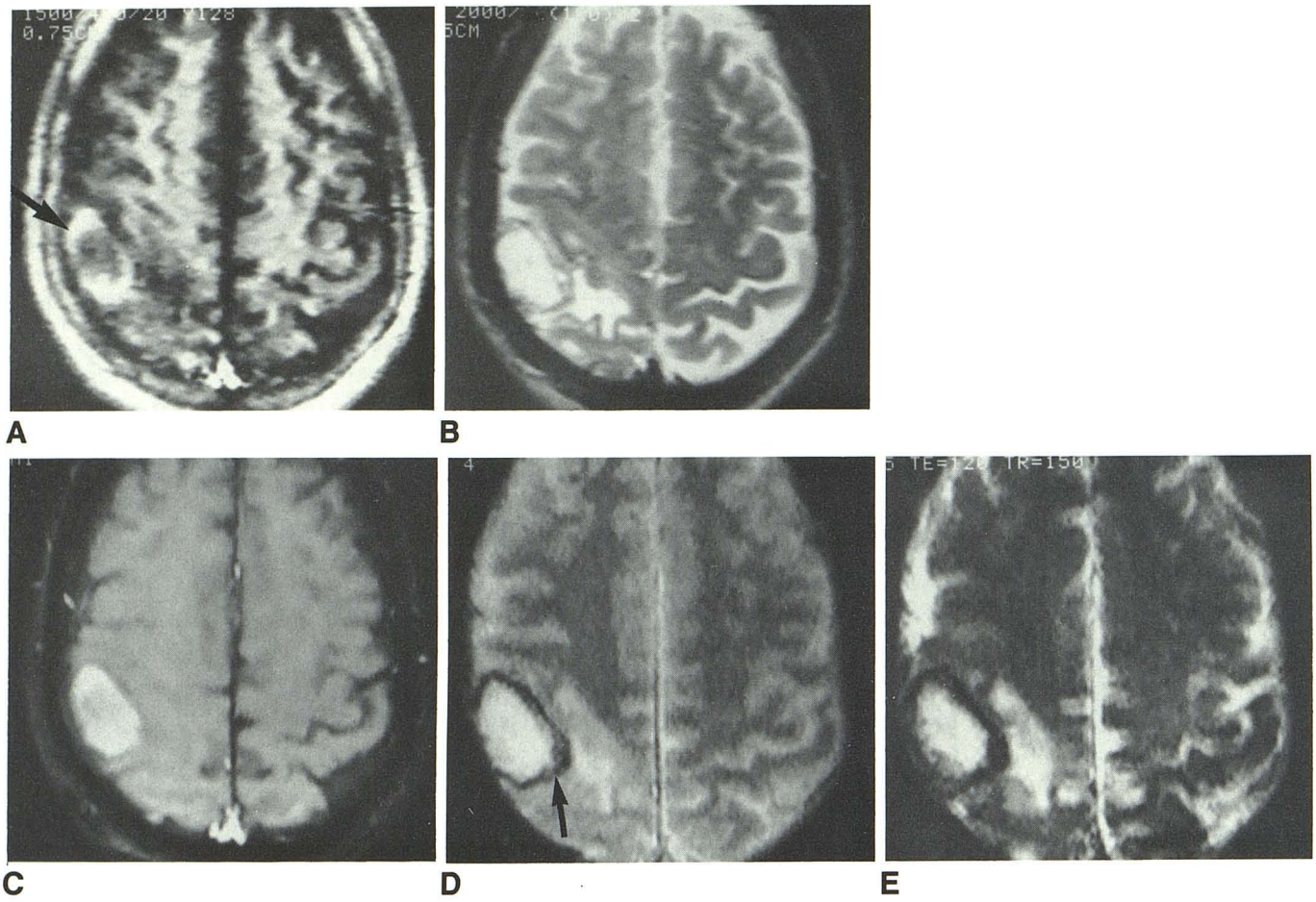

Fig. 3.—Patient with 4-week-old right parietal hemorrhage. **A**, T1-weighted IR image shows hyperintense ring (*arrow*), presumably due to paramagnetic methemoglobin. **B**, Heavily T2-weighted SE image (TE = 120 msec) shows no definite evidence of a magnetic susceptibility effect. **C**, T1-weighted PS image (TE = 16 msec) shows marked hyperintensity of lesion. Again note prominent flow enhancement. **D**, T2-weighted PS image (TE = 50 msec) shows moderately thick halo of very low intensity due to magnetic susceptibility gradient between hemorrhage and normal brain. **E**, More T2-weighted PS image (TE = 120 msec) shows still more prominent halo.

(Fig. 4D) Also noted were phase shifts at the air-soft tissue interfaces between sphenoid sinus and normal brain. Pituitary hemorrhage appeared hyperintense on T1- and T2-weighted SE images, but hypointense on T2-weighted PS images (Fig. 5). A liver hematoma was also markedly hypointense on T2-weighted PS images.

Nonhemorrhagic lesions had similar appearances on SE and PS images. None of the lesions showed any evidence of central hypointensity or low-intensity halo to suggest a magnetic susceptibility effect (Fig. 6).

Discussion

Magnetic susceptibility effects in acute and nonacute hemorrhages are easily detected on intermediate-field MR images. This has been demonstrated by a new method that permits T1- and T2-weighted images to be obtained in as little as 10 sec.

The diagnosis of nonacute hemorrhage is generally not difficult on lower-field images because of the striking hyperintensity on T1-weighted images. However, this finding, which is thought to be due to methemoglobin formation, is not seen in acute hemorrhage. High-field MR images have been shown to be sensitive to magnetic susceptibility changes that are present in acute hemorrhage [1]. In acute hematomas, these changes have been attributed to the presence of paramagnetic deoxyhemoglobin, and in nonacute hematomas to the presence of hemosiderin.

It has been suggested that images obtained at lower field strengths are insensitive to these magnetic susceptibility effects, and therefore cannot be used to detect acute hemorrhage [2]. In fact, the failure of previous investigators to observe these effects at intermediate and low fields is likely due to the use of an inappropriate technique. The spin-echo pulse sequence is designed to eliminate the effects of magnetic field inhomogeneities [7]. Because of this insensitivity, the quality of SE images is generally superior to PS images; however, SE images are also less sensitive to inhomogeneities due to magnetic susceptibility variations.

Variations in magnetic susceptibility due to the presence of paramagnetic material leads to changes in the local magnetic field within and immediately surrounding the hemorrhage.

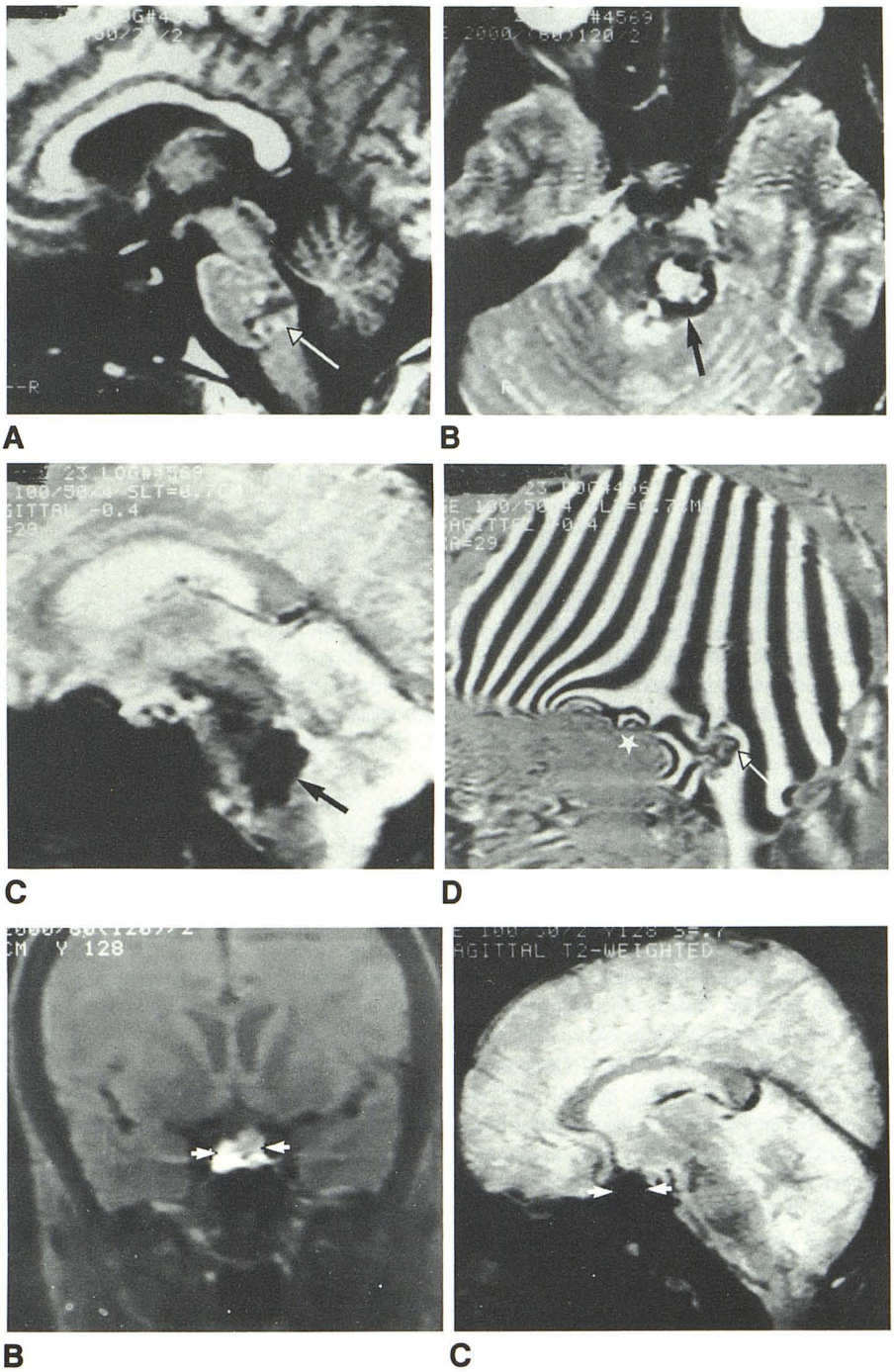

Fig. 4.—Patient with pontine arteriovenous malformation occult to angiography. **A**, T1-weighted IR image shows speckled hyperintensity (*arrow*) within lesion, consistent with methemoglobin. **B**, T2-weighted SE image (TE = 120 msec) shows hyperintense central region; hypointense halo (*arrow*) is consistent with magnetic susceptibility effect. **C**, T2-weighted PS image (TE = 50 msec) shows marked hypointensity of entire lesion (*arrow*). **D**, Phase-sensitive zebra-stripe reconstruction shows marked phase shifts in region of partially thrombosed AVM (*arrow*). Phase shifts are noted at air-soft tissue interfaces between sphenoid sinus (*asterisk*) and brain.

Fig. 5.—Patient imaged with postpartum pituitary apoplexy imaged 1 week following ictus. **A**, T1-weighted sagittal IR image shows hyperintensity consistent with methemoglobin formation (*arrowheads*). **B**, T2-weighted coronal SE image (TE = 60 msec) shows moderate hyperintensity (*arrowheads*). **C**, T2-weighted sagittal PS image (TE = 30 msec) shows marked hypointensity of lesion (*arrowheads*).

These magnetic field variations have two consequences. First, diffusion of protons through regions of varying magnetic field during the NMR experiment will act to diminish spin-echo signal intensity; refocusing of signal during spin-echoes assumes each proton sees a constant (time-invariant) magnetic field. Because variations in the field are proportional to the magnetic field strength, this effect is more pronounced at higher magnetic fields and accounts for the changes seen on conventional SE images. However, since water does not diffuse very far during a single TE period, most protons see a relatively constant magnetic field, even if their neighbors see a slightly different field, and thus signal changes on SE images can be subtle, especially for short TE and lower field strengths. Variations in magnetic field within a hemorrhage

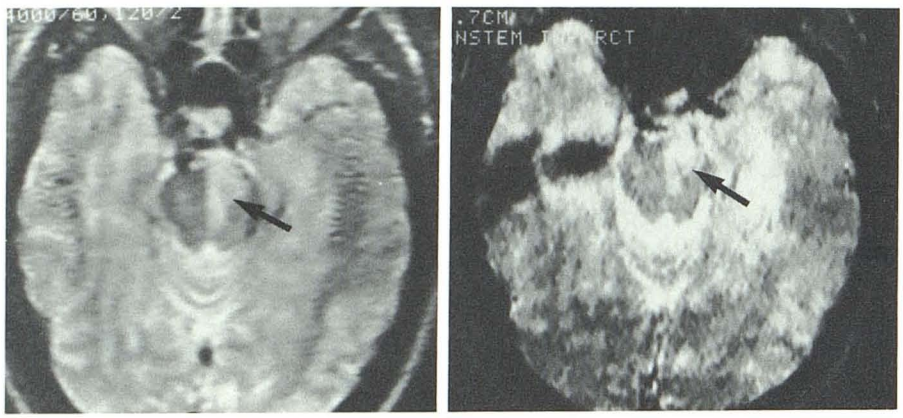

Fig. 6.—Patient with nonhemorrhagic pontine infarct. **A**, T2-weighted SE image (TE = 120 msec) shows hyperintense infarct (*arrow*). **B**, T2-weighted PS image (TE = 50 msec) again shows hyperintense lesion (*arrow*). There is no evidence of any magnetic susceptibility effect within or around the infarct.

will have a more direct effect on signal intensity if gradient-refocused, PS pulse sequences are used. In essence, signal decay is governed by the field variations or line width within each voxel, and is thus characterized by the time constant T2*, which is sensitive to the effects of magnetic field inhomogeneities, rather than by T2. In this case, even stationary protons will be dephased relative to their neighbors since no spin-echo is used. This effect will be, in general, larger than diffusion-related phenomena. In our data, the much greater signal loss on PS vs SE images at similar TE times indicates that this is indeed the case.

Although magnetic susceptibility effects in hemorrhage will be detected more sensitively at higher fields, these effects should be detectable at lower fields by using longer TE. In several of our cases the presence of hemorrhage could be suggested by the presence of areas of hypointensity on T2-weighted SE images acquired with TE of 120 msec (Figs. 2 and 4). This finding has also been described by other investigators working with an intermediate-field system [9]. However, worsening signal noise eventually limits the maximum TE that can be used. We have overcome the limited sensitivity of the SE sequence by using gradient-echoes, which, as illustrated in Figure 1, are far more sensitive to magnetic susceptibility effects than are spin-echoes. In all cases of hemorrhage we were able to show striking hypointensity within and around the lesions. The sensitivity of PS images to these effects can be increased simply by increasing TE, until a point is reached at which the increased T2* effects at longer TE are balanced by worsening signal noise. In our study, even PS 150/120 images showed adequate signal noise (Fig. 3), as well as striking magnetic susceptibility effects.

All hemorrhages in our study showed a prominent halo of marked hypointensity on T2-weighted PS images. Although this halo has been related to the presence of hemosiderin [1], our results suggest that it can represent a boundary effect between two regions of differing magnetic susceptibility (hemorrhage vs normal brain), and does not always imply the presence of hemosiderin.

Conventional magnitude images are insensitive to the intervoxel phase-shifts associated with hemorrhage-induced field variations. Phase-sensitive reconstructions can be used to detect these phase shifts directly, so as to further enhance the sensitivity of our technique to the presence of bulk magnetic susceptibility effects. Another potential application of this technique would be for mapping iron distribution in the brain, which has hitherto only been feasible on high-field systems [10].

Our method should be still more powerful on a high-field system. Using this method, one should be able to detect far smaller quantities of iron at an earlier stage in disease processes than has been possible using conventional SE techniques. However, the inability to characterize hemorrhage on lower-field systems has been a major argument in favor of high-field systems. Our results suggest that, by use of the appropriate imaging technique, hemorrhage can be characterized as well or better at intermediate fields than has hitherto been demonstrated on high-field systems.

ACKNOWLEDGMENTS

We thank Randy Lauffer and Alice Vincent for helpful discussions and for preparation of phantoms.

REFERENCES

1. Gomori J, Grossman RI, Goldberg HI, et al. Intracranial hematomas: imaging by high-field MR. *Radiology* **1985**;157:87–93
2. Zimmerman RA, Bilaniuk LT, Grossman RI, et al. Resistive NMR of intracranial hematomas. *Neuroradiology* **1985**;27:16–20
3. DeLaPaz RL, New PFJ, Buonanno FS, et al. NMR imaging of intracranial hemorrhage. *J Comput Assist Tomogr* **1984**;8:599–607
4. Bydder GM, Young IR. Clinical use of the partial saturation and saturation recovery sequences in MR imaging. *J Comput Assist Tomogr* **1985**;9:1020–1032
5. Wedeen VJ, Rosen BR, Chesler D, Brady TJ. MR velocity imaging by phase display. *J Comput Assist Tomogr* **1985**;9:530–536
6. Renshaw PF, Owen CS, McLaughlin AC, et al. Ferromagnetic contrast agents: a new approach. *Mag Res Med* **1986**;3:217–225
7. Hahn EL. Spin echoes. *Physiol Rev* **1950**;80:580–594
8. James TL. *NMR in biochemistry*. New York: Academic Press, **1975**:165
9. Zimmerman RD, Deck MDF. Intracranial hematomas: imaging by high-field MR. (Letter to the Editor). *Radiology* **1986**;159:565
10. Drayer B, Burger P, Darwin R, Riederer S, Herfkens R, Johnson GA. Magnetic resonance imaging of brain iron. *AJNR* **1986**;7:373–380